

Estimation of the energy loss at the blades in rowing: Common assumptions revisited

MATHIJS HOFMIJSTER, JOS DE KONING, & A. J. VAN SOEST

Faculty of Human Movement Sciences, Vrije Universiteit Amsterdam, Amsterdam, Netherlands

(Accepted 22 May 2010)

Abstract

In rowing, power is inevitably lost as kinetic energy is imparted to the water during push-off with the blades. Power loss is estimated from reconstructed blade kinetics and kinematics. Traditionally, it is assumed that the oar is completely rigid and that force acts strictly perpendicular to the blade. The aim of the present study was to evaluate how reconstructed blade kinematics, kinetics, and average power loss are affected by these assumptions. A calibration experiment with instrumented oars and oarlocks was performed to establish relations between measured signals and oar deformation and blade force. Next, an on-water experiment was performed with a single female world-class rower rowing at constant racing pace in an instrumented scull. Blade kinematics, kinetics, and power loss under different assumptions (rigid versus deformable oars; absence or presence of a blade force component parallel to the oar) were reconstructed. Estimated power losses at the blades are 18% higher when parallel blade force is incorporated. Incorporating oar deformation affects reconstructed blade kinematics and instantaneous power loss, but has no effect on estimation of power losses at the blades. Assumptions on oar deformation and blade force direction have implications for the reconstructed blade kinetics and kinematics. Neglecting parallel blade forces leads to a substantial underestimation of power losses at the blades.

Keywords: *Blade force, oar deformation, efficiency of propulsion, aquatic locomotion*

Introduction

Competitive rowing races take place over a distance of 2000 m. By pulling on the oars, a rower causes a reaction force of the water on the oar blades, which propels the boat–oars–rower system against the water resistance force acting on the boat. As is the case in any aquatic mode of transport, it is inevitable that energy is lost to the water in the generation of the propulsive force: kinetic energy is imparted to the water at the blades. This energy is “lost” in the sense that it is unrelated to the energy needed to overcome drag. In previous work, we showed that the power equation is a helpful tool to analyse rowing performance (Hofmijster, Landman, Smith, & van Soest, 2007; Hofmijster, van Soest, & de Koning, 2008).

Considering steady-state rowing as a periodic behaviour, the average net mechanical power terms for the boat–oars–rower system are related as follows:

$$P_{\text{rower}} = -(P_{\text{drag}} + P_{\text{blade}})$$

Note that all three terms in this equation concern averages over a complete rowing cycle. Strictly

speaking, P_{rower} represents the average value of the net mechanical power produced/dissipated within this non-rigid system. In fact, this term captures the net mechanical power produced by the rower, averaged over a full cycle. As argued elsewhere (Hofmijster et al., 2007), acceleration and deceleration of boat and rower affect the instantaneous power flow, but vanish when the net mechanical power equation is averaged over a full cycle of periodic steady-state rowing. In the equation above, P_{drag} refers to the average mechanical power dissipated through water and air drag on hull and rower. Similarly, P_{blade} refers to the average mechanical power lost at the blades. Ideally, a rower simultaneously maximizes net mechanical power production and minimizes power losses at the blades.

The characteristics of the oar and the shape of the blade are important determinants of the power loss at the blades (Affeld, Schichl, & Ziemann, 1993; Caplan & Gardner, 2007a,c). An optimal oar–blade combination allows the rower to generate a high propulsive force without it resulting in high power loss at the blades. Blade force and power have been

measured under controlled conditions, where the blade was immersed at different orientations in a flow tank. However, as already noted by Barré and Kobus (1998), the validity of data obtained under steady-state conditions is currently unclear because in reality the flow around the blades is non-steady. A promising new technique for estimation of blade force is based on a finite element method referred to as computational fluid dynamics (Coppel, Gardner, Caplan, & Hargreaves, 2008; Leroyer, Barré, Kobus, & Visonneau, 2008). With current computation power, high-resolution simulations, under non-steady conditions, are feasible. Computational fluid dynamics therefore is a potentially powerful tool for the evaluation of new blade designs.

The only way to validate results obtained from flow tank experiments and from computational fluid dynamics simulations is to compare these to blade force and blade power data based on measurements under realistic conditions. Until now, blade kinetics and kinematics in on-water rowing were reconstructed from measurements of the oar angle in the horizontal plane and either the moment on the oar (Affeld et al., 1993; Baudouin & Hawkins, 2004; Kleshnev, 1999; Smith & Spinks, 1998) or the force on the pin perpendicular to the oar (Hofmijster et al., 2007). From these data, blade force and blade kinematics were reconstructed assuming that the oar is rigid and that the blade force is always perpendicular to the blade orientation (Baudouin & Hawkins, 2002; Brearly & de Mestre, 1996; Cabrera, Ruina, & Kleshnev, 2006; Hofmijster et al., 2007; Sanderson & Martindale, 1986; Zatsiorsky & Yakunin, 1991). Furthermore, it has often been assumed that the point of application of the blade force is located at a fixed distance from the pin (Baudouin & Hawkins, 2004; Sanderson & Martindale, 1986), usually at the centre of the blade (Affeld et al., 1993; Baudouin & Hawkins, 2002; Brearly & de Mestre, 1996; Cabrera et al., 2006; Hofmijster et al., 2007; Zatsiorsky & Yakunin, 1991). Instantaneous blade power can be calculated by taking the dot product of the vectors of blade force and the velocity of its point of application. In previous work, power losses at the blades were reported to be in the order of 20–30% of total mechanical power (Affeld et al., 1993; Hofmijster et al., 2007; Kleshnev, 1999).

The assumption that the oar is rigid (Baudouin & Hawkins, 2002; Brearly & de Mestre, 1996; Cabrera et al., 2006; Hofmijster et al., 2007; Sanderson & Martindale, 1986; Zatsiorsky & Yakunin, 1991) is clearly unrealistic, as considerable deformation of the oar can be observed by eye during rowing competitions. Neglecting this deformation leads to errors in the reconstructed trajectory of both the centre and the orientation of the blade. The consequences of these errors for the reconstructed blade power are

currently unclear. Similarly, the assumption that the blade force acts perpendicular to the blade (Baudouin & Hawkins, 2002; Brearly & de Mestre, 1996; Cabrera et al., 2006; Hofmijster et al., 2007; Sanderson & Martindale, 1986; Zatsiorsky & Yakunin, 1991) is questionable, because the combination of translation of the hull and rotation of the oar results in a blade trajectory for which the angle of attack is by no means perpendicular to the blade at all times. Consequently, there is a power loss associated with the currently unknown force component that is parallel to the blade. Macrossan (2008) mentioned that both the deflection of the blade force vector from the normal direction as well as oar bending would have an effect on the efficiency of the blade (Macrossan, 2008). The third assumption in the reconstruction of blade power concerns the point of application of the blade force. Recent work using computational fluid dynamics (Kinoshita, Miyashita, Kobayashi, & Hino, 2008) has revealed different blade pressure distributions at different angles of attack. These results imply that the assumption that the point of application of the blade force always lies at the centre of the blade may also need to be reconsidered.

In summary, there is reason to question the accuracy of the assumptions underlying current estimates of blade power losses in rowing. It is the aim of this study to evaluate the adequacy of two of these assumptions. In particular, oar deformation and parallel blade force during racing conditions is reported and we evaluate how reconstructed blade kinematics, kinetics, and power loss are affected by assumptions regarding oar rigidity and blade force direction.

Methods

Outline of the study

In this study, the effects of assumptions about oar rigidity and blade force direction on blade kinematics, blade kinetics and, most importantly, power loss at the blades were evaluated. First, a calibration experiment with custom-made instrumented oars and oarlocks was performed, aimed at establishing the relations between measured signals on the one hand and oar deformation and blade force (F_{blade} , in two dimensions) on the other. Next, an on-water experiment was performed in which a single world-class rower rowed at a constant racing pace. From the measured signals, blade kinematics, blade kinetics, and power loss at the blades under different assumptions (rigid versus deformable oars; absence or presence of a blade force component parallel to the oar) were reconstructed. The focus of this study was a comparison of results of different methods of

analysis, thus the statistical analysis of the data is in terms of descriptive measures.

Participant and protocol of the on-water rowing experiment

The single participant in this study was a world-class female rower aged 23 years (height 1.73 m, body mass 70 kg). The participant provided written informed consent and the study was approved by the local ethics committee. The participant rowed a distance of 500 m at racing pace (i.e. 30–32 strokes per minute), starting from zero boat velocity, in an instrumented single scull. Remote-controlled data acquisition was started at zero boat velocity and was terminated slightly after the 500-m line was passed. Elapsed time after 100, 250, and 500 m was recorded using a stopwatch.

Measurement system

An instrumented racing single scull (Filippi, Italy) was used. Data from the impeller (Nielsen Kellerman, USA) mounted underneath the hull was sampled by the data acquisition system (see below). In addition, hull acceleration in the direction of travel was measured using an accelerometer (ADXL204, Analog Devices, USA). The oars were the commonly used “big blades” (Concept II, USA), the outboard parts of which were cut in order to mount custom-built oar shaft sensors, such that the centre of the sensors was 0.35 m from the pivoting point of the oar (Figure 1). Each sensor consisted of two individual strain-gauge force sensors, mounted at 45° relative to the length axis of the unloaded oar shaft. As explained below, the oar shaft sensors were used to reconstruct the blade force component that is parallel to the face of the oarlock (F_{parallel}). To keep the oars mechanically balanced, a counterweight was placed at equal distance from the pivoting point on the inboard section of the oar. The horizontal-plane angle between the parts of the oars

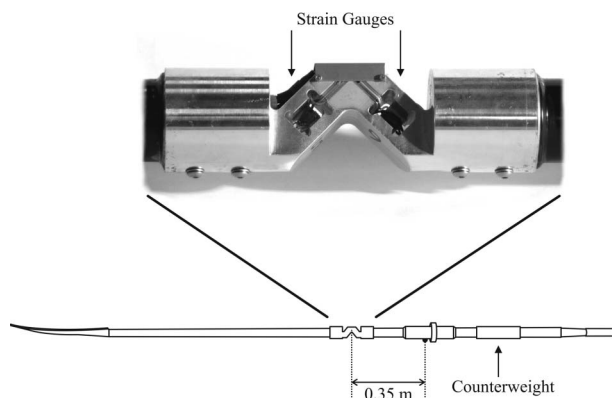


Figure 1. Oarshaft sensor.

near the oarlocks and the boat (referred to as φ_{oar} in this study) was measured using servo-potentiometers (FCP12-AC, Feteris Components, Netherlands) mounted in each of the oarlocks. Force on the pin (F_{pin}) was measured using custom-made strain-gauge force transducers integrated in each of the oarlocks (Figure 2). The oarlock sensor data were used to reconstruct the component of the force between oar and oarlock that is perpendicular to the face of the oarlocks (see below). All sensor data were sampled at 1000 Hz and stored on-board the boat on a data acquisition computer (PC 104 Prometheus, Diamond Systems, USA). After the experiment, the data were transferred to a PC for offline analysis. The same system was used for data acquisition during the calibration experiment (see below).

Calibration procedure

The aim of the calibration procedure was to derive gains that allow reconstruction of oar deformation and net blade force components (in the frame of reference shown in Figure 3) from the custom force sensors at oarlock and oar shaft. With that aim in mind, a horizontal-plane calibration experiment was carried out in the laboratory, in which oarlock and oar shaft custom force sensor signals were sampled at 1 kHz while an external horizontal force was applied to the centre of the blade through a cable. The cable was pulled by the experimenter via an independently calibrated 1-DOF force transducer (AST, Germany). The force applied to the blade ranged between 0 and 150 N, the expected range during on-water rowing, and was sampled synchronized with the oarlock and



Figure 2. Oarlock sensor, including force and angle transducers.

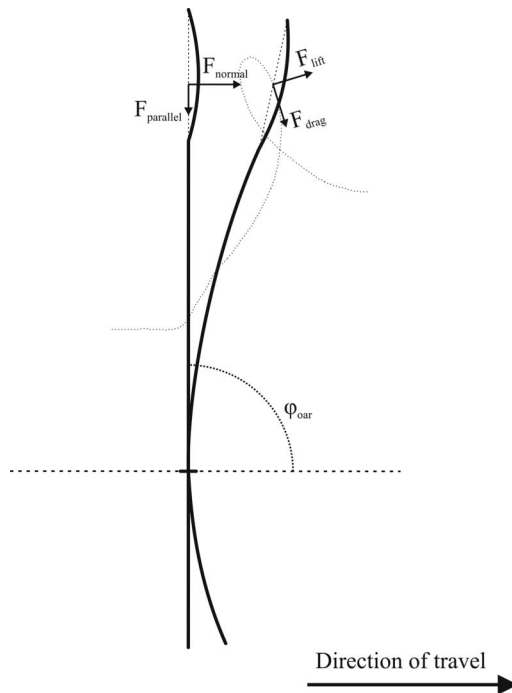


Figure 3. Schematic representation of the oar during the stroke phase. The (unrealistic) rigid oar and the oar under deformation are both shown. Parallel blade forces and perpendicular blade forces are oriented along the main axes of an oarlock-bound frame of reference. Lift and drag forces on the blade are oriented along the main axes of a (moving) frame of reference aligned with the movement direction of the centre of the blade. The angle of the oar in the horizontal plane is indicated by φ_{oar} .

oar shaft custom force sensor signals. Simultaneously, oar kinematics were measured using an Optotrak 3020 position sensor (Optotrak, Northern Digital, Canada); see Figure 4 for the location of the active infrared markers. Calculation of the custom force sensor gains was based on calibration trials in which inward, perpendicular, and outward forces were applied to the blade. Data from a separate trial during which blade force magnitude and direction were varied quasi-randomly were used to validate the calibration parameters (this trial is referred to as the validation trial). During all trials, the oarlock pin was fixed, allowing free oar rotation around a vertical axis, and the oar handle was supported at the assumed point of application of the handle force (see below). Both oar deformation and blade force components are described in a frame of reference aligned with the face of the oarlock (see Figure 3).

In the reconstruction of relevant variables described below, two assumptions were made. First, it was assumed that the oar dynamics can be neglected; consequently, a quasi-static approach was used in which oar deformation and blade force were reconstructed from the measured force data. Second, assumptions were made regarding the point of application of the handle force and the net blade

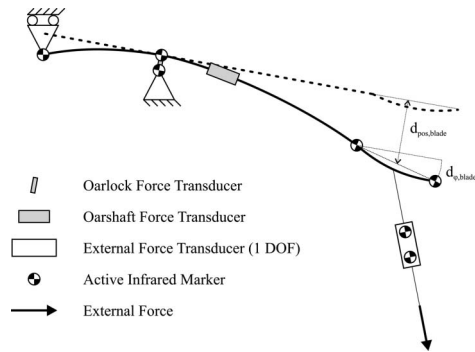


Figure 4. Calibration set-up. The arrow indicates the quasi-randomly applied external force. The pin and handle were supported. The handle was able to translate freely from left to right; the pin with oarlock was able to rotate freely. Oar deformation was described in terms of $d_{\text{pos,blade}}$ and $d_{\varphi,\text{blade}}$, as defined in the figure.

force during on-water rowing, as we were unable to reconstruct these points of application from the data.

Oar deformation was described in terms of deflection of the centre of the blade ($d_{\text{pos,blade}}$) and orientation change of the blade ($d_{\varphi,\text{blade}}$), as illustrated in Figure 4. These quantities were found to be linearly related to the oarlock custom force sensor data. Least-squares optimal custom force sensor gains were calculated from the data obtained during the calibration trials. Using these gains, the oar deformation in the validation trial was predicted and subsequently compared with the kinematic data from the validation trial (Figures 5a and 5b). This resulted in r^2 of 0.82 (starboard) and 0.96 (port) for deflection of the centre of the blade and 0.92 (starboard) and 0.97 (port) for the change in orientation of the blade. More detailed analysis (data not shown) revealed that the relatively low value for the explained variation in deflection of the blade for the starboard oar was caused by noise in the position data (obtained through the Optotrak system) for this trial.

Perpendicular blade force could be reconstructed most reliably from the oarlock custom force sensor data. It was assumed that handle force is applied at 0.85 m from the oarlock, and that net blade force is applied at the geometric centre of the blade (1.80 m from the oarlock). During the calibration and validation trials, the forces were indeed applied at these points. Least-squares optimal force sensor gains were calculated from the data obtained during the calibration trials, using a linear model. Using these force sensor gains, the perpendicular force in the validation trial was predicted and subsequently compared with the actual perpendicular force as obtained from the independent force transducer (Figure 6). This resulted in r^2 of 1.00 (both starboard and port). Parallel blade forces were reconstructed from oarshaft and oarlock sensor signals in a similar manner as the reconstruction of the perpendicular

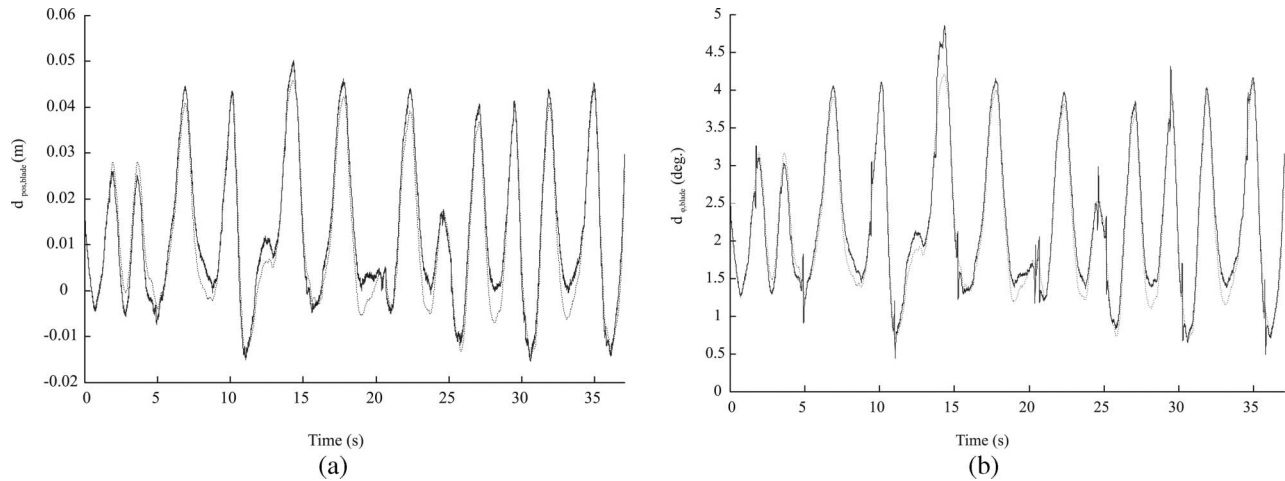


Figure 5. Results of the calibration trials for $d_{\text{pos,blade}}$ (a) and $d_{\phi,\text{blade}}$ (b) for the port side oar. Solid lines indicate values calculated from Optotrak data, dashed lines indicate values reconstructed from the pin force sensor. The figures display the measured values plotted against the estimated values. There was some unexpected noise (“spikes” in the solid curve) in the measured $d_{\phi,\text{blade}}$ signal, caused by noise in the signal of one of the position markers. As this noise is high frequency in nature, no effect on the quality of the fit is expected.

blades forces. Comparison of predicted and actual parallel forces again resulted in r^2 of 1.00 (both starboard and port).

Data analysis for the on-water experiment

Kinematics. From the combination of impeller data and stopwatch data (elapsed time after 100, 250, and 500 m), the boat displacement per full impeller revolution (which was in the order of 0.03 m) was calculated for each section of the 500-m trial. Using these values, the average boat velocity was calculated for each full stroke cycle. Instantaneous boat velocity was calculated by numerically integrating the acceleration signal over stroke duration, using the average velocity calculated from the impeller data as the integration constant. Boat displacement was calculated by integrating instantaneous boat velocity over time. Blade position and velocity (relative to the world) were calculated from the combination of boat kinematics relative to the world and blade kinematics relative to the boat as reconstructed from the oar angle and oar deformation.

Kinetics. Blade force components in the frame of reference shown in Figure 3 were reconstructed using the calibration parameters obtained in the calibration experiment (see above). During the recovery phase (identified as the phase where $|F_{\text{pin}}| < 15$ N and $d\phi_{\text{oar}}/dt < 0$), the blade force was set to zero. For further data analysis, the reconstructed blade force vector was decomposed in a component in the direction of the velocity vector of the centre of the blade, which can be seen as a drag force ($F_{\text{drag,blade}}$), and a component perpendicular to that, which can be seen as a lift force ($F_{\text{lift,blade}}$; see Figure 3).

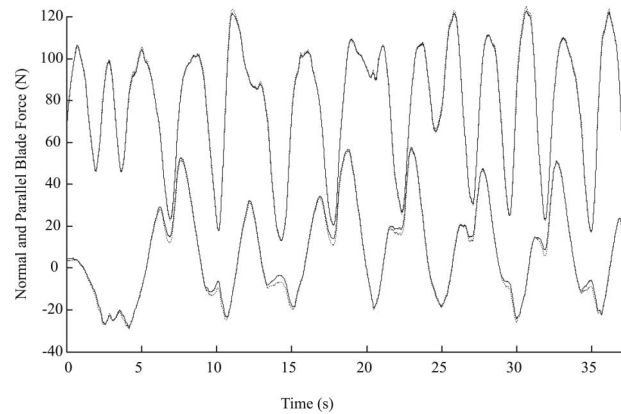


Figure 6. Results of the calibration trials for perpendicular blade forces (top curves) and parallel blade forces (bottom curves). Solid lines indicate measured values, dashed lines predicted values. The figures display the measured values plotted against the estimated values. Data correspond to those used in Figure 5.

Energetics. Instantaneous power lost to the water at each blade ($P_{\text{blade, instantaneous}}$) was calculated as the dot product of the reconstructed blade force vector and the reconstructed velocity vector of the centre of the blade, relative to the world. As there is no power associated with the lift force, instantaneous power losses at the blade can also be calculated as the product of drag force at the blade and blade velocity. Instantaneous blade power was calculated under four different combinations of assumptions. Regarding the reconstructed blade force, parallel blade force was or was not assumed to be zero. Regarding the reconstructed blade kinematics, oar deformation was or was not assumed. Instantaneous blade power was numerically integrated over stroke time to obtain energy loss to the water at the blades for each stroke

(W_{blade}); dividing this quantity by stroke cycle duration yielded average blade power; note that this average is calculated over the full stroke cycle, including the recovery phase.

Descriptive statistics

For the analyses of blade kinetics and kinematics, 10 consecutive strokes cycles in steady-state conditions were selected. When applicable, values were averaged over the 10 stroke cycle period. For the four combinations of assumptions that are analysed, the 95% confidence interval for power losses at the blades was calculated.

Results

Blade kinematics

The blade kinematics for the rigid oar assumption and for the situation where oar deformation was taken into account are shown in Figure 7. For both conditions, the mean kinematics and the range of values observed for the 10 selected strokes are displayed. The repeatability between the strokes is high. Overall, the reconstructed path of the oar lies more towards the bow when oar deformation is taken into account. Figure 8 shows blade angle relative to the boat for the rigid and deformable oar assumptions. Figures 8 and 9 show that the effect of taking

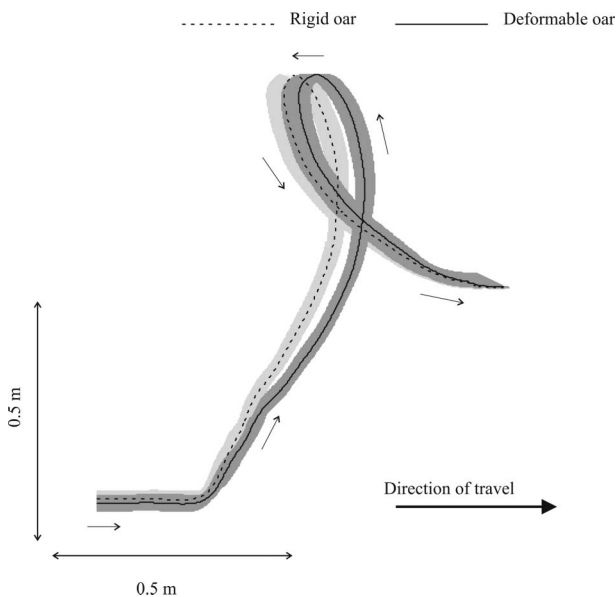


Figure 7. Effect of assumptions about oar rigidity on the kinematics of the blade (port side oar). The dashed line represents the reconstructed path of the centre of the blade, assuming a rigid oar. The solid line represents the reconstructed path of the centre of the blade when oar deformation is taken into account. The shaded area indicates the range of values found for the 10 consecutive strokes on which this figure is based. Small arrows indicate the direction of movement.

oar deformation into account has a substantial effect on the reconstructed blade kinematics.

Blade force

Parallel blade force as measured by the oar shaft force sensors is shown in Figure 9. These data indicate that during the stroke phase, parallel blade force is non-negligible, acting inwards on the blade during the first half of the stroke, and acting outwards during the second half of the stroke (Figure 9). Of interest is the fact that parallel blade force is non-zero when the blade is perpendicular to the boat (approximately at time = 0.6; see Figure 8). When still water is assumed, the angle of

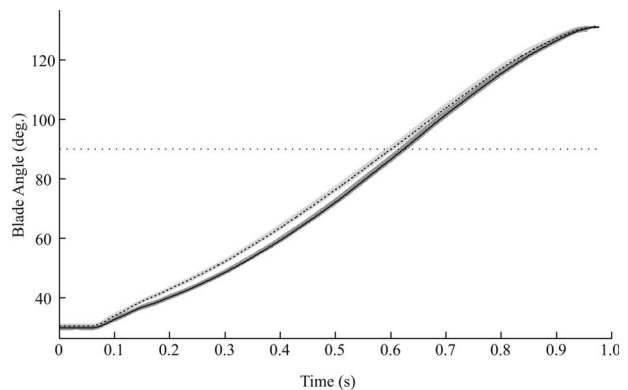


Figure 8. Effect of assumptions about oar rigidity on the angle of the blade relative to the boat. The shaded area indicates the range of values found for the same 10 strokes as used in Figure 7. For each of the selected strokes, the start of the stroke phase is set at $t = 0$. The blade is perpendicular to the direction of travel of the boat at a blade angle of 90° , which is indicated by the dashed horizontal line.

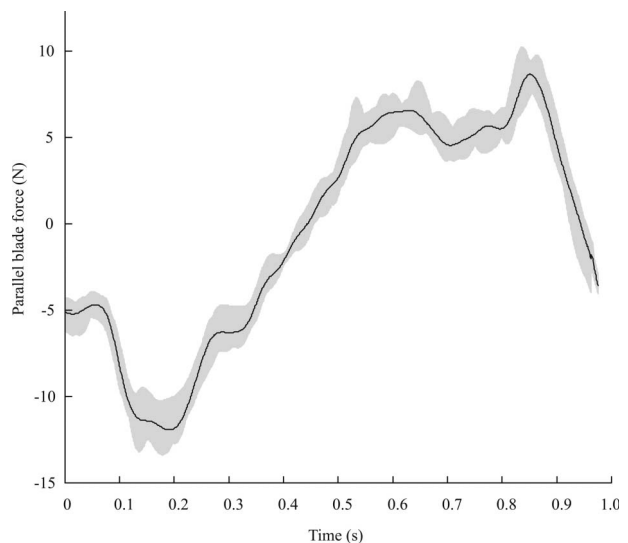


Figure 9. Parallel blade force. The shaded area indicates the range of values found for the same 10 strokes as used in Figure 7. For each of the selected strokes, the start of the stroke phase is set at $t = 0$.

attack would be 90° at this moment in time, and only a force component perpendicular to the blade would be expected. In our view, this could suggest three things: (1) water is accelerated outwards in the first half of the stroke; (2) asymmetry of the blade causes deviation of the direction of the blade force vector away from the normal direction; or (3) specific blade (hydro)dynamics result in a measurement error that was not accounted for in the calibration procedure.

Total blade force was decomposed into drag force and lift force on the blade. Note that this decomposition depends both on the incorporation of oar deformation and the incorporation of parallel blade force. Figure 10 highlights the effect of incorporating oar deformation and parallel blade force on the decomposition of blade force in drag force and lift force on the blade. It can be seen that when it is assumed that the oar is rigid and parallel blade force is zero, an underestimation of drag force on the blade is made in the first and last part of the stroke, whereas drag force on the blade is slightly overestimated during the middle part of the stroke. Lift force appears to be overestimated during the second half of the stroke when it is assumed that the oar is rigid and parallel blade force is not present. Figures 11a and 11b show the same variables for one typical stroke, including (at discrete intervals) blade orientation and the blade force components.

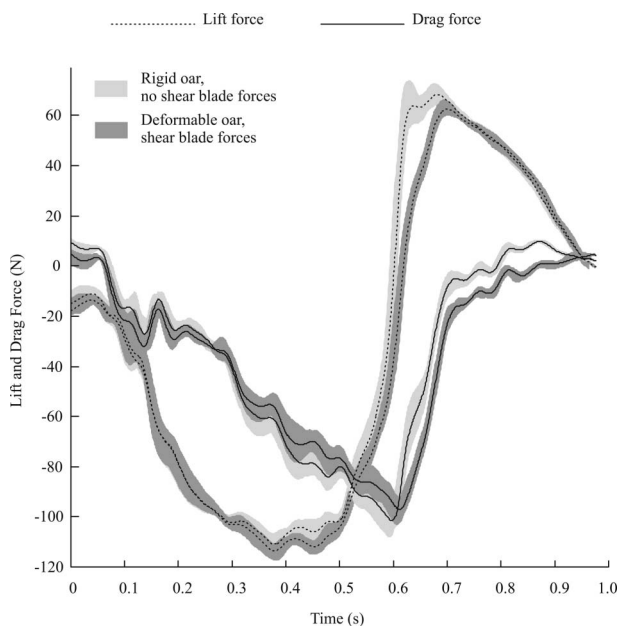


Figure 10. Effect of neglecting parallel blade forces on the decomposition of total blade force in F_{blade} and F_{drag} . The shaded area indicates the range of values found for the same 10 strokes as used in Figure 7. For each of the selected strokes, the start of the stroke phase is set at $t = 0$.

Power lost at the blades

Table I shows power losses at the blades and work lost at the blades for both oars calculated for the four situations described. The table shows that taking oar deformation into account has very little effect on the values calculated for power losses at the blades and work lost at the blades. When parallel blade force is taken into account, however, the estimated values for both power losses at the blades and work lost at the blades are 18% higher. This implies that the assumption that blade force only acts perpendicular to the blade results in a substantial underestimation of the power lost to drag. In Figure 12, instantaneous power loss at the blade is compared between the situation in which oar deformation and parallel blade force are assumed to be absent and the situation where oar deformation and parallel blade force are taken into account. Figure 12 shows that especially at the beginning and the end of the stroke, instantaneous power loss at the blade is underestimated when oar deformation and parallel blade force are ignored. This is due primarily to an underestimation of the drag forces on the blade at the beginning and end of the stroke (as can be seen in Figure 10) and not so much to a different oar velocity profile resulting from incorporating oar deformation. This follows from the fact that power loss at the blade has similar values between the situation of rigid oar assumption and the situation where oar deformation is taken into account (see Table I).

Discussion

The results of this study indicate that the rigid-oar assumption and the no-parallel-blade-force assumption that were commonly adopted in the reconstruction of blade kinematics and kinetics in previous studies (Baudouin & Hawkins, 2002; Brearly & de Mestre, 1996; Cabrera et al., 2006; Hofmijster et al., 2007; Sanderson & Martindale, 1986; Zatsiorsky & Yakunin, 1991) are untenable. Regarding kinetics, it was found that neglecting parallel blade forces results in an underestimation of power losses at the blades of almost 20%. Regarding kinematics, it was found that the reconstructed blade kinematics are substantially affected when oar deformation is taken into account. Both the reconstructed path of the centre of the blade in the water and the angle of the blade in relation to the boat are substantially different from the actual situation when the oar is assumed to be rigid. Somewhat surprisingly, these differences in blade kinematics had a negligible effect on the estimated average power loss at the blades. This is at odds with Macrossan (2008), who found higher blade efficiencies when the blade force vector was non-normal, and lower blade efficiencies when oar bending was

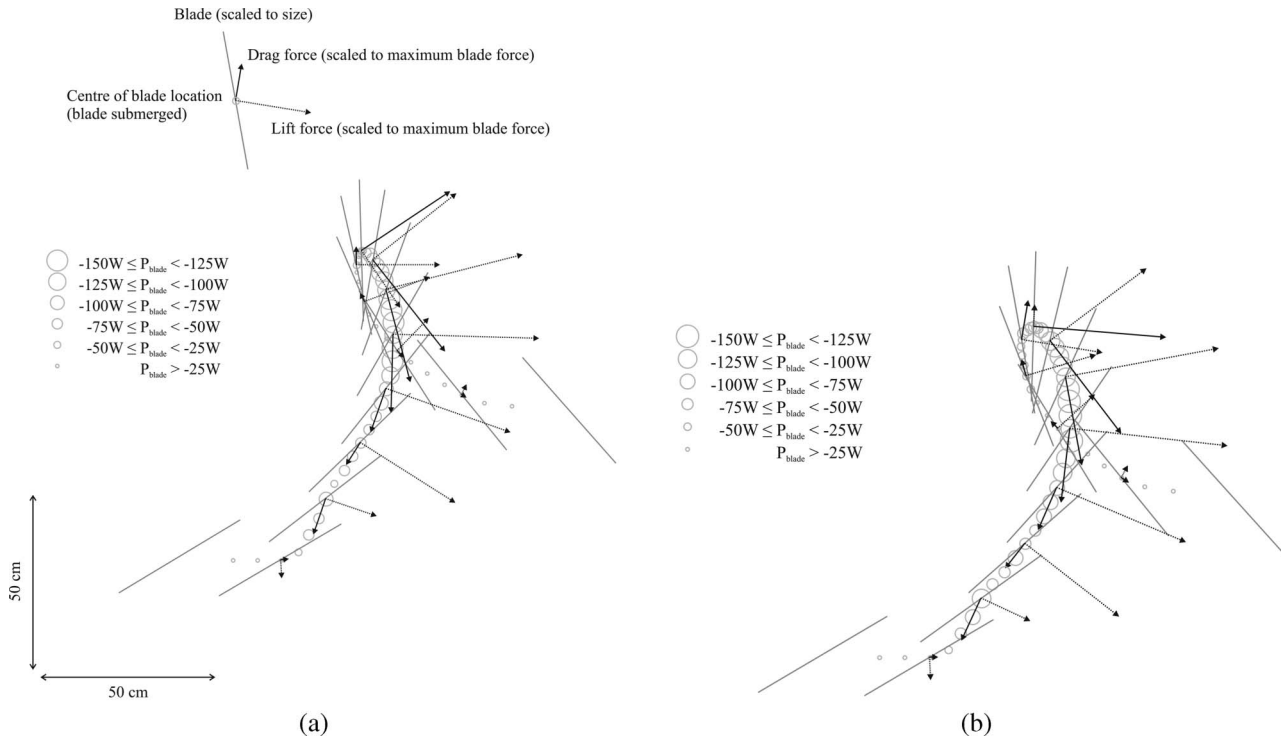


Figure 11. Comparison of estimated blade kinematics for two situations: (a) the oar is assumed to be rigid, blade force acts only perpendicular to the blade; (b) the oar is deformable and F_{parallel} is also present. This figure is based on a typical example of a stroke. The position of the blade is plotted at 0.02-s intervals, and the size of the circle provides an indication of the power dissipation at the blade at that point in time. Lift force (dashed arrow) and drag force (solid arrow) on the blade (grey line) are plotted at 0.08-s intervals.

Table I. Effect of assumptions regarding rigidity of the oar and direction of the force vector at the blades on the estimated values of power and work lost at the blades and on the 95% confidence interval for power and work lost at the blades (in parentheses).

	Oar deformation neglected	Oar deformation incorporated
Parallel blade forces neglected		
P_{blades} (W)	-45.7 (-49.8 to -41.5)	-45.8 (-50.0 to -41.6)
W_{blades} (J)	-91.9 (-99.5 to -84.4)	-92.2 (-99.8 to -84.5)
Parallel blade forces incorporated		
P_{blades} (W)	-53.7 (-59.7 to -49.6)	-53.9 (-58.1 to -49.7)
W_{blades} (J)	-108.1 (-115.7 to -100.5)	-108.4 (-116.0 to -100.8)

taken into account. A part of the explanation for these discrepancies could be that Macrosson used a slightly different definition of “efficiency” than is customary in our laboratory (e.g. Hofmijster et al., 2007). More detailed analysis indicated that incorporating oar deformation in the reconstruction of blade kinematics had an effect on instantaneous power loss at the blades; however, on average, power loss at the blade was not affected. Although we have elucidated the effect of the rigid-oar assumption and the no-parallel-blade-force assumption on the corre-

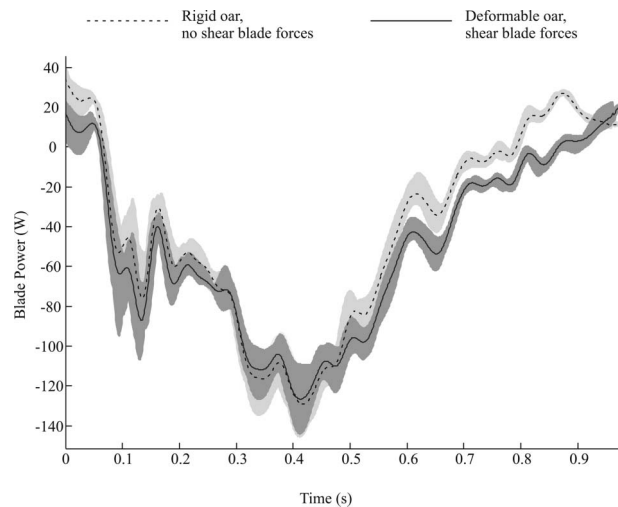


Figure 12. Comparison of estimated $P_{\text{blade, instantaneous}}$ for two situations. In the first situation (dashed line), the oar is assumed to be rigid and a parallel blade force is assumed to be absent. In the second situation (solid line), the oar is assumed to be deformable, and F_{parallel} is assumed to be present. The shaded area indicates the range of values found for the 10 selected strokes.

sponding value for power losses at the blades, we would like to stress at this point that this study in no way supports the value of oar deformation and/or parallel blade force. This is because the actual values of these quantities were not varied; all values for

power losses at the blades were calculated from the same data set, using different assumptions affecting the reconstructed blade kinematics.

This study is based on data obtained from a single participant who was an expert rower. It is possible that the effects of the rigid-oar assumption and the no-parallel-blade-force assumption vary between different rowers. However, although the actual hydrodynamics around the blade are rather complex, the kinematics of oar and blade are fairly straightforward. Oars will bend when forces are exerted on handle and blade, and similar blade trajectories have been reported in several independent studies in the past (Affeld et al., 1993; Hofmijster et al., 2007; Zatsiorsky & Yakunin, 1991). There is no reason to expect that the consequences of different sets of assumptions, which were the topic of this study, are highly sensitive to the relatively small differences in movement execution between expert rowers. Therefore, it is in our view acceptable that this study is based on data obtained from a single participant. The extent to which the amount of power lost at the blades differs between rowers, and the relation between movement execution and these power losses are interesting topics for future research. This study points out that in such studies, at least parallel blade forces and oar bending should be taken into account.

Although the magnitude of the parallel blade force seems small, the contribution of this force to the drag force is not negligible. This is especially true at the start and end of the stroke phase, where the drag force is almost parallel to the blade. In these parts of the stroke, power losses are substantially underestimated when parallel blade forces are neglected. From our results, it would appear that it is favourable to somehow minimize this force component during the first part of the stroke phase. It is unclear whether this is possible by either changing the blade design or by adapting the rower's technique. Of note is a study by Brearley and de Mestre (2000), who found considerable increases in efficiency when the blade is tilted forward with respect to the shaft. This would offset any negative effects caused by oar bending in the mid-part of the stroke (Brearley & de Mestre, 2000). A possible problem with simulation studies like these is that it is assumed that the force input (delivered by the rower) is the same for each situation and as such independent of oar design.

In this study, two commonly held assumptions regarding blade kinetics and kinematics were assessed. Due to technical limitations, we were not able to investigate the validity of the assumption regarding the point of application of the blade force. In line with earlier work by ourselves and others (Baudouin & Hawkins, 2002; Hofmijster et al., 2007; Zatsiorsky & Yakunin, 1991), we assumed the point of application of the blade force to be at the centre of

the blade. However, simulation results obtained from computational fluid dynamics models suggest that the location of the point of application changes during the stroke from outwards at the start of the stroke to inwards at the finish of the stroke (Kinoshita et al., 2008). To get a first impression of the sensitivity of our results for the location of the assumed point of application, we recalculated all our results for a point of application located either 0.10 m more inward or 0.10 m more outward. Most importantly in the context of the present study, our conclusions regarding assumptions on oar rigidity and blade force direction are not at all sensitive to the assumed point of application. However, it was also found that the value of power lost at the blades is highly sensitive for the assumed point of application; in other words, the values for power loss at the blades reported in this study depend strongly on the assumed point of application. In our view, this indicates that there is a need for experimental determination of the point of application under racing conditions.

Another aspect of the bending of the oar that was not assessed in this study is the energy needed to deform the oar. If the oars are perfectly elastic, this energy, being a fraction of the mechanical energy produced by the rower, is stored and subsequently "given back" in a later stage of the rowing cycle. Otherwise, a part of this energy is lost, meaning that this would be an additional power loss term. The magnitude of this term is unknown, but it is obvious that for optimal performance the energy dissipated in the oars should be minimal.

Computational fluid dynamics is a promising technique for future research on blade hydrodynamics. The direction of the force vector, as well as its point of application, can be obtained from reliable simulations. For future modeling using computational fluid dynamics, obtaining the correct kinematic data for the blades is important. Computational fluid dynamics models reconstruct hydrodynamic forces as a function of the prescribed movement of the blade in the water (Coppel, Gardner, Caplan, & Hargreaves, 2009; Leroyer et al., 2008). For these models to produce meaningful results, it is therefore crucial that the correct kinematic data are used as input. Thus, when reconstructing on-water kinematics of the blades from measurements of oar angle and boat displacement, it is important to take the deformation of the oar into account.

Previous estimates of power losses at the blades were in the order of 20–30% of the rower's power output (Affeld et al., 1993; Hofmijster et al., 2007; Kleshnev, 1999). Results of this study indicate that power losses at the blades are in fact substantially higher. Thus, rowers spend a substantial part of their power in the process of generating a propulsive force on the blade. We therefore expect improvements in

blade design to result in a substantial improvement in performance. The most recent marked improvement in blade design dates back to 1992, when “Macon” blades were replaced by big blades. Recently, Caplan and Gardner (2007c) suggested a small improvement in blade efficiency when a more rectangular blade shape is used. However, as also is pointed out in a follow-up study by the same group (Coppel et al., 2008), at this point transfer of their results to actual on-water rowing is questionable. Tests were done under steady-state conditions and a scale model was used. Consequently, tests were performed at a Froude number that is different to that in reality. Again, this points out the need for reliable field measurements.

Several authors stated that lift forces are the main contributors to the propulsive force during the first and last part of the stroke phase, whereas drag forces are the main contributors to the propulsion in the mid-part of the stroke phase (Baudouin & Hawkins, 2002; Caplan & Gardner, 2007b). As can be seen from Figures 11a and 11b, our data do not support this view. Both figures show that, irrespective of the assumptions used, lift force is the main contributor to the propulsion for almost the entire stroke phase.

In summary, our study shows that assumptions on oar deformation and the direction of blade force have large implications for the reconstructed blade kinetics and kinematics. Most importantly, neglecting parallel blade forces leads to a substantial underestimation of the average power lost at the blades. Energy losses during push-off appear to be even larger than previously expected. The magnitude of these losses calls for future research on the possibilities of minimizing power losses at the blades, for instance by optimizing blade design or improving the rower’s technique.

Acknowledgements

This study was partially funded by NOC*NSF and TNO. We would like to thank Concept 2 Benelux for unconditionally providing us with a single scull and oars. We would like to thank the technical staff, in particular Erik Clay, Guido Cox and Huybert van der Stadt, for all their efforts concerning the measurement system. We would also like to thank Ellen Maas for her help with the experiments.

References

Affeld, K., Schichl, K., & Ziemann, A. (1993). Assessment of rowing efficiency. *International Journal of Sports Medicine*, *14*, S39–S41.

Barré, S., & Kobus, J.-M. (1998). New facilities for measurement and modelling of hydrodynamic loads on oar blades. In S. J. Haake (Ed.), *The engineering of sport: Design and development*. (pp. 251–259). Oxford: Blackwell Science.

Baudouin, A., & Hawkins, D. (2002). A biomechanical review of factors affecting rowing performance. *British Journal of Sports Medicine*, *36*, 396–402.

Baudouin, A., & Hawkins, D. (2004). Investigation of biomechanical factors affecting rowing performance. *Journal of Biomechanics*, *37*, 959–976.

Brearily, M. N., & de Mestre, N. J. (1996). Modelling the rowing stroke and increasing its efficiency. In *Proceedings of the Third Conference on Mathematics and Computers in Sport* (pp. 35–46), Bond University, Queensland, Australia.

Brearily, M. N., & de Mestre, N. J. (2000). Improving the efficiency of racing shell oars. *Mathematical Gazette*, *84*, 405–414.

Cabrera, D., Ruina, A., & Kleshnev, V. (2006). A simple 1+ dimensional model of rowing mimics observed forces and motions. *Human Movement Science*, *25*, 192–220.

Caplan, N., & Gardner, T. N. (2007a). A fluid dynamic investigation of the big-blade and macon oar blade designs in rowing propulsion. *Journal of Sports Sciences*, *25*, 643–650.

Caplan, N., & Gardner, T. N. (2007b). A mathematical model of the oar blade–water interaction in rowing. *Journal of Sports Sciences*, *25*, 1025–1034.

Caplan, N., & Gardner, T. N. (2007c). Optimization of oar blade design for improved performance in rowing. *Journal of Sports Sciences*, *25*, 1471–1478.

Coppel, A., Gardner, T., Caplan, N., & Hargreaves, D. (2008). Numerical modelling of the flow around rowing oar blades. In M. Estivalet & P. Brisson (Eds.), *The engineering of sport* (pp. 353–361). Paris: Springer.

Coppel, A., Gardner, T. N., Caplan, N., & Hargreaves, D. (2009). Simulating the fluid dynamic behaviour of oar blades in competition rowing. *Proceedings of the Institution of Mechanical Engineers, Part P: Journal of Sports Engineering Technology*, *224*, 25–35.

Hofmijster, M. J., Landman, E. H. J., Smith, R. M., & van Soest, A. J. (2007). Effect of stroke rate on the distribution of net mechanical power in rowing. *Journal of Sports Sciences*, *25*, 403–411.

Hofmijster, M. J., van Soest, A. J., & de Koning, J. J. (2008). Rowing skill affects power loss on a modified rowing ergometer. *Medicine and Science in Sports and Exercise*, *40*, 1101–1110.

Kinoshita, T., Miyashita, M., Kobayashi, H., & Hino, T. (2008). Rowing velocity prediction program with estimating hydrodynamic load acting on an oar blade. In N. Kato & S. Kamimura (Eds.), *Biomechanics of swimming and flying, fluid dynamics, biomimetic robots, and sports science* (pp. 345–359). Tokyo: Springer.

Kleshnev, V. (1999). Propulsive efficiency of rowing. In *Scientific Proceedings: ISBS ‘99: XVII International Symposium on Biomechanics in Sports* (pp. 69–72), Perth School of Biomedical and Sports Science, Edith Cowan University, Perth, WA.

Leroyer, A., Barré, S., Kobus, J.-M., & Visonneau, M. (2008). Experimental and numerical investigations of the flow around an oar blade. *Journal of Marine Science and Technology*, *13*, 1–15.

Macrossan, M. N. (2008). The direction of the water force on a rowing blade and its effect on efficiency. *Mechanical Engineering Report No. 2008/03*. URL: http://espace.uq.edu.au/eserv/UQ:134269/MER2008_03.pdf

Sanderson, B., & Martindale, W. (1986). Towards optimizing rowing technique. *Medicine and Science in Sports and Exercise*, *18*, 454–468.

Smith, R. M., & Spinks, W. L. (1998). A system for the biomechanical assessment of rowing performance (ROWSYS). *Journal of Human Movement Studies*, *34*, 141–157.

Zatsiorsky, V. M., & Yakunin, N. (1991). Mechanics and biomechanics of rowing: A review. *International Journal of Sport Biomechanics*, *7*, 229–281.